Karlsruhe Institute of Technology

Hochschule Karlsruhe
Technik und Wirtschaft
UNIVERSITY OF APPLIED SCIENCES

Extreme Scale Phase-Field Simulations of Sintering Processes

J. Hötzer, H. Hierl, M. Seiz, A. Reiter and B. Nestler

INSTITUTE OF APPLIED MATERIALS - COMPUTATIONAL MATERIALS SCIENCE

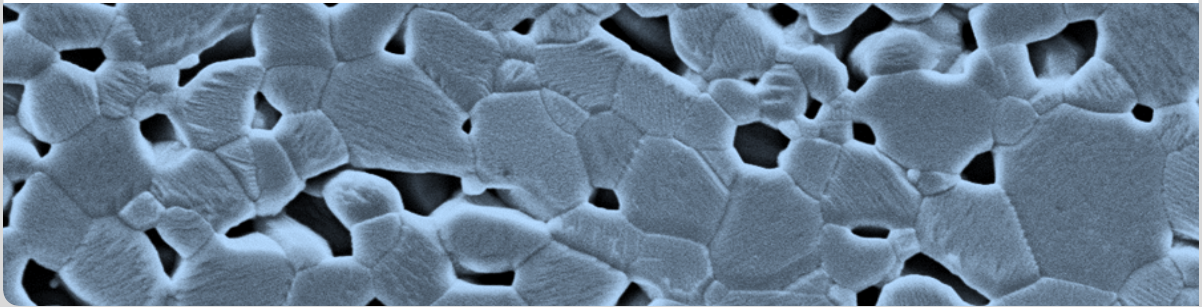

Part I: Institute

http://zkm.de/en/event/2015/06/schlosslichtspiele

The Group “High Performance Materials Computing and Data Science”

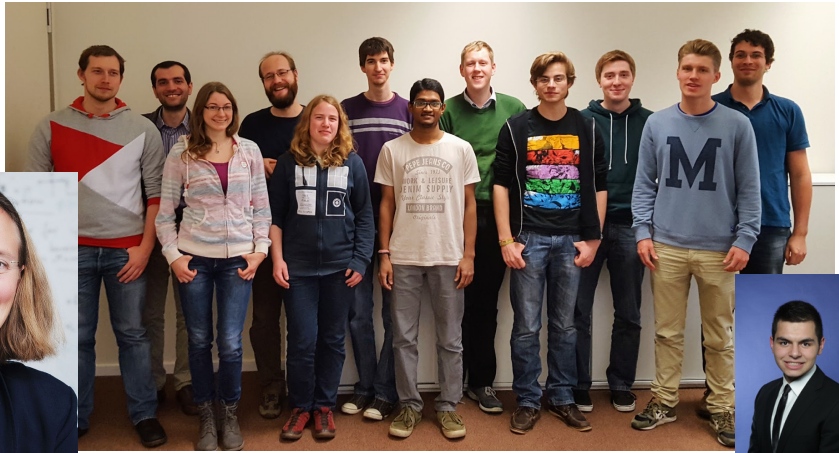

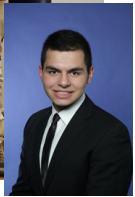

Part II: Motivation

What do these pictures have in common?

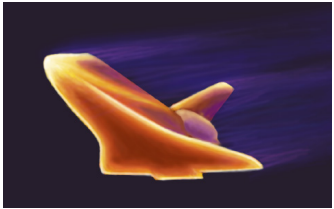

https://upload.wikimedia.org/wikipedia/commons/6/6a/Sparkplug.jpg

What do these pictures have in common?

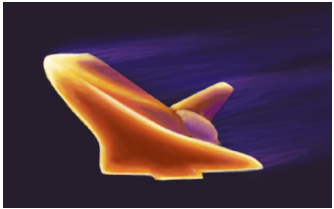

all structures result from the same process:
sintering

https://upload.wikimedia.org/wikipedia/commons/6/6a/Sparkplug.jpg

What do these pictures have in common?

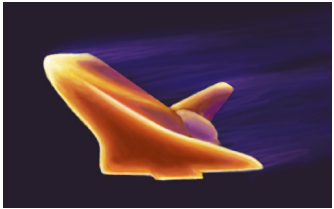

all structures result from the same process:
sintering

high performance materials require defined properties

https://upload.wikimedia.org/wikipedia/commons/6/6a/Sparkplug.jpg

Motivation - Material properties

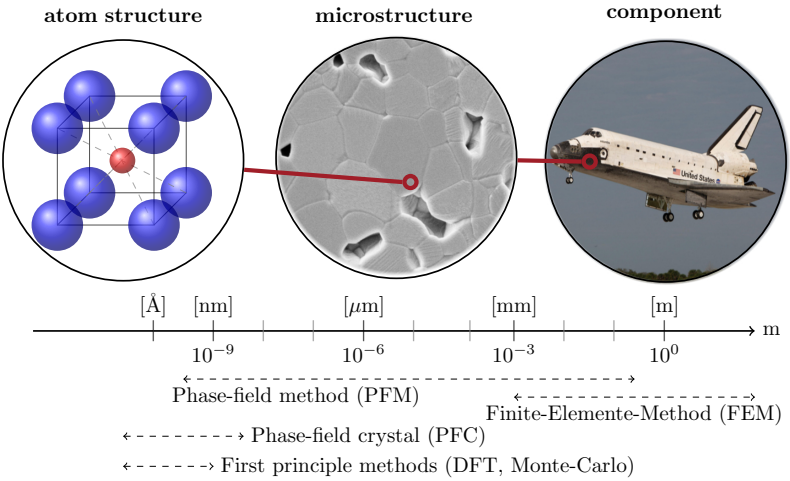

- **chemical elements** and **microstructure** determine the **properties** of the component
  $\Rightarrow$ controlling the **microstructure evolution** = controlling the **material properties**

Motivation - Material properties

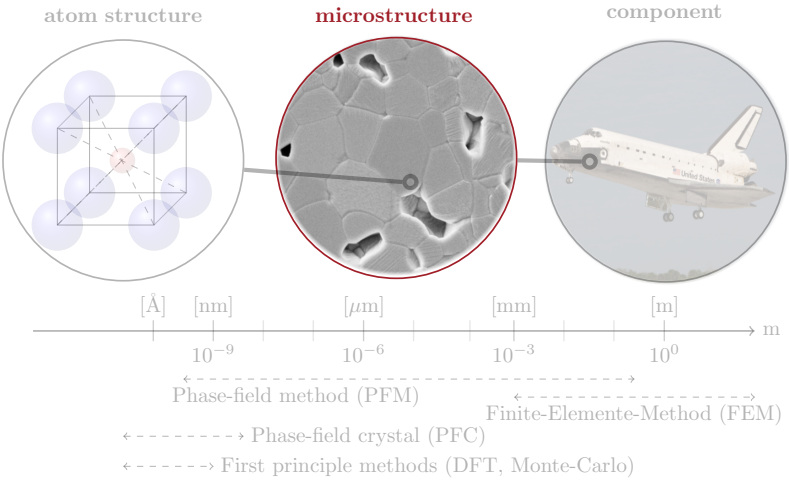

- **chemical elements** and **microstructure** determine the **properties** of the component
  $\Rightarrow$ controlling the **microstructure evolution** = controlling the **material properties**

Sintering process

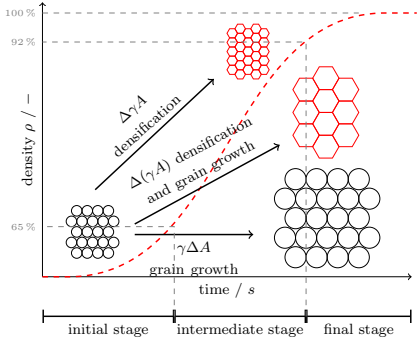

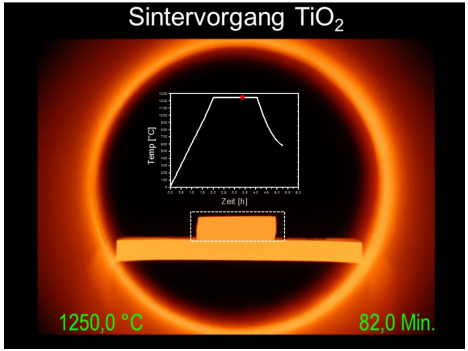

- three stages of sintering
  - initial: evolution of sintering necks
  - intermediate: **densification** of green body
  - final: **grain growth**

⇒ difficult to predict and control microstructure

Video: IAM-KWT, KIT

Part III: Phase-field model for sintering

Phase-field method

- **minimization** of the **total energy** in a system under constraints
- **coupling** with different **physical quantities** (e.g. concentration, temperature, ...)
- **phase-field vector** $\phi = (\phi_1, \phi_2, ..., \phi_N)^T$
- **order-parameter** ϕ_α describes the volume fraction of the phases with different properties, e.g. orientation, ...
- modeling of a defined **diffuse interface** between the phases

  $\Rightarrow$ for numerical resolution ≈ 10 cells required

  $\Rightarrow$ high resolution of the structures required

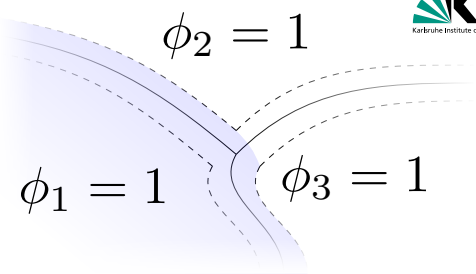

Phase-field method

- **minimization** of the **total energy** in a system under constraints
- **coupling** with different **physical quantities** (e.g. concentration, temperature, ...)
- **phase-field vector** $\phi = (\phi_1, \phi_2, ..., \phi_N)^T$
- **order-parameter** ϕ_α describes the volume fraction of the phases with different properties, e.g. orientation, ...
- modeling of a defined **diffuse interface** between the phases
  - $\Rightarrow$ for numerical resolution ≈ 10 cells required
  - $\Rightarrow$ high resolution of the structures required

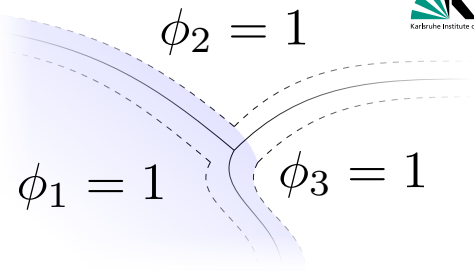

Phase-field method

- **minimization** of the **total energy** in a system under constraints
- **coupling** with different **physical quantities** (e.g. concentration, temperature, ...)
- **phase-field vector** $\boldsymbol{\phi} = (\phi_1, \phi_2, ..., \phi_N)^T$
- **order-parameter** ϕ_α describes the volume fraction of the phases with different properties, e.g. orientation, ...
- modeling of a defined **diffuse interface** between the phases
  - $\Rightarrow$ for numerical resolution ≈ 10 cells required
  - $\Rightarrow$ high resolution of the structures required

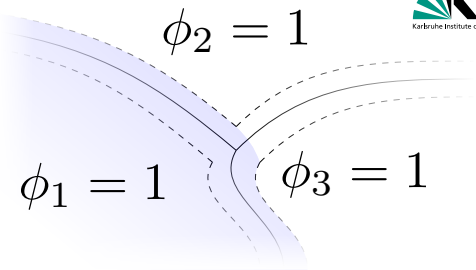

Phase-field method

- **minimization** of the **total energy** in a system under constraints
- **coupling** with different **physical quantities** (e.g. concentration, temperature, ...)
- **phase-field vector** $\boldsymbol{\phi} = (\phi_1, \phi_2, ..., \phi_N)^T$
- **order-parameter** ϕ_α describes the volume fraction of the phases with different properties, e.g. orientation, ...
- modeling of a defined **diffuse interface** between the phases
  - $\Rightarrow$ for numerical resolution ≈ 10 cells required
  - $\Rightarrow$ high resolution of the structures required

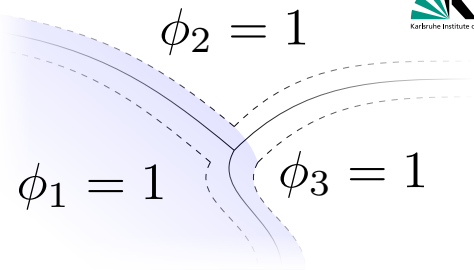

Phase-field method

- **minimization** of the **total energy** in a system under constraints
- **coupling** with different **physical quantities** (e.g. concentration, temperature, ...)
- **phase-field vector** $\phi = (\phi_1, \phi_2, ..., \phi_N)^T$
- **order-parameter** ϕ_α describes the volume fraction of the phases with different properties, e.g. orientation, ...
- modeling of a defined **diffuse interface** between the phases
  - ⇒ for numerical resolution ≈ 10 cells required
  - ⇒ high resolution of the structures required

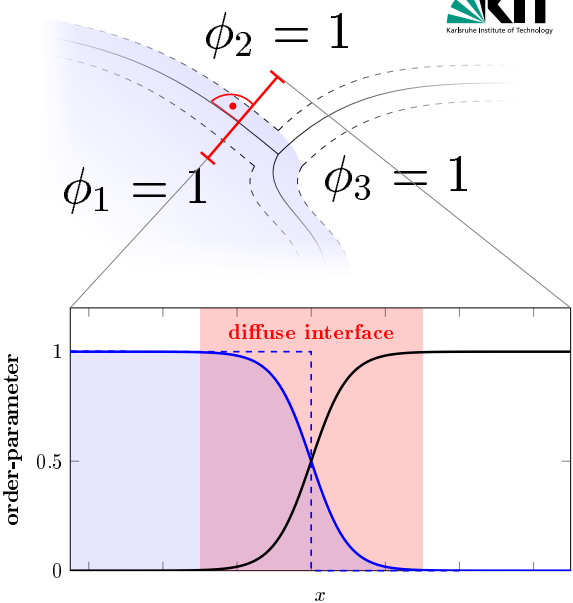

Phase-field method

- **minimization** of the **total energy** in a system under constraints
- **coupling** with different **physical quantities** (e.g. concentration, temperature, ...)
- **phase-field vector** $\phi = (\phi_1, \phi_2, ..., \phi_N)^T$
- **order-parameter** ϕ_α describes the volume fraction of the phases with different properties, e.g. orientation, ...
- modeling of a defined **diffuse interface** between the phases
  - ⇒ for numerical resolution ≈ 10 cells required
  - ⇒ high resolution of the structures required

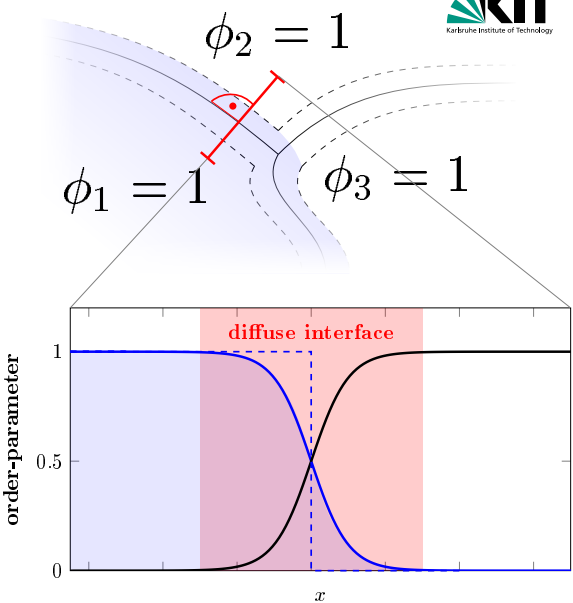

Phase-field method

- **minimization** of the **total energy** in a system under constraints
- **coupling** with different **physical quantities** (e.g. concentration, temperature, ...)
- **phase-field vector** $\phi = (\phi_1, \phi_2, ..., \phi_N)^T$
- **order-parameter** ϕ_α describes the volume fraction of the phases with different properties, e.g. orientation, ...
- modeling of a defined **diffuse interface** between the phases
  - ⇒ for numerical resolution ≈ 10 cells required
  - ⇒ high resolution of the structures required

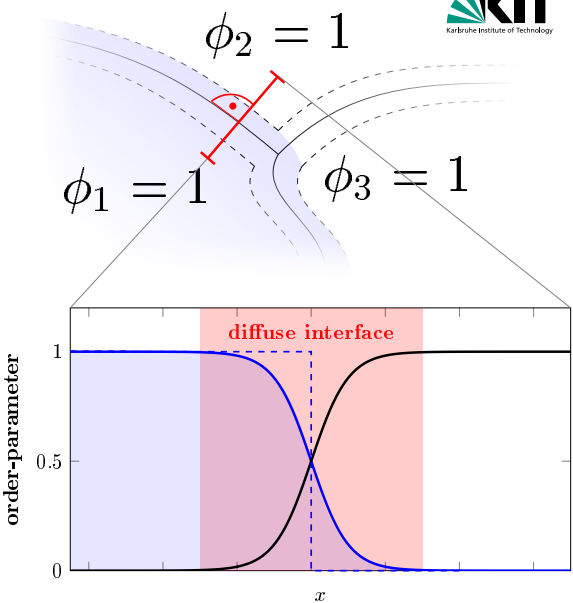

Phase-field model for solid state sintering

- **phase-field model** based on grand potential approach
  - evolution of phase-fields $\partial_t \phi_\alpha$
  - evolution of chemical potentials $\partial_t \mu$
  - constant temperature
- different **diffusion mechanisms**: surface (5), grain boundary (2) and volume diffusion (1,3,4,6)
- **arbitrary** number **phases/grains**
- **optimized** on different levels
- massive-parallel PACE3D framework

$\Rightarrow$ **efficient simulation** of large domains

Hötzer et al. Phase-field simulation of solid state sintering, Acta Materialia (2018)

Phase-field model for solid state sintering

- **phase-field model** based on grand potential approach
  - evolution of phase-fields $\partial_t \phi_\alpha$
  - evolution of chemical potentials $\partial_t \mu$
  - constant temperature
- different **diffusion mechanisms**: surface (5), grain boundary (2) and volume diffusion (1,3,4,6)
- **arbitrary** number **phases/grains**
- **optimized** on different levels
- massive-parallel PACE3D framework

⇒ **efficient simulation** of large domains

$$\tau\varepsilon\frac{\partial\phi_\alpha}{\partial t} = \underbrace{-\varepsilon\left(\frac{\partial a(\phi,\nabla\phi)}{\partial\phi_\alpha} - \nabla\cdot\frac{\partial a(\phi,\nabla\phi)}{\partial\nabla\phi_\alpha}\right) - \frac{1}{\varepsilon}\frac{\partial\omega(\phi)}{\partial\phi_\alpha}}_{\text{interface contribution } := \text{rhsl}_\alpha}$$

$$\underbrace{-\frac{\partial\psi(\phi,\mu,T)}{\partial\phi_\alpha}}_{\text{driving force } := \text{rhsf}_\alpha} - \frac{1}{N}\sum_{\beta=1}^{N}(\text{rhsl}_\beta + \text{rhsf}_\beta)$$

Hötzer et al. Phase-field simulation of solid state sintering, Acta Materialia (2018)

Phase-field model for solid state sintering

- **phase-field model** based on grand potential approach
  - evolution of phase-fields $\partial_t \phi_\alpha$
  - evolution of chemical potentials $\partial_t \boldsymbol{\mu}$
  - constant temperature
- different **diffusion mechanisms**: surface (5), grain boundary (2) and volume diffusion (1,3,4,6)
- **arbitrary** number **phases/grains**
- **optimized** on different levels
- massive-parallel PACE3D framework

⇒ **efficient simulation** of large domains

$$\tau\varepsilon\frac{\partial\phi_\alpha}{\partial t} = \underbrace{-\varepsilon\left(\frac{\partial a(\phi,\nabla\phi)}{\partial\phi_\alpha} - \nabla\cdot\frac{\partial a(\phi,\nabla\phi)}{\partial\nabla\phi_\alpha}\right) - \frac{1}{\varepsilon}\frac{\partial\omega(\phi)}{\partial\phi_\alpha}}_{\text{interface contribution } :=\text{rhsl}_\alpha}$$

$$\underbrace{-\frac{\partial\psi(\phi,\boldsymbol{\mu},T)}{\partial\phi_\alpha}}_{\text{driving force } :=\text{rhsf}_\alpha} - \frac{1}{N}\sum_{\beta=1}^{N}(\text{rhsl}_\beta + \text{rhsf}_\beta)$$

$$\frac{\partial\boldsymbol{\mu}}{\partial t} = \left[\sum_{\alpha=1}^{N} h_\alpha(\vec{\phi})\left(\frac{\partial\vec{c}_\alpha(\boldsymbol{\mu},T)}{\partial\boldsymbol{\mu}}\right)\right]^{-1} \left(\nabla\cdot\left(\boldsymbol{M}(\vec{\phi},\boldsymbol{\mu},T)\nabla\boldsymbol{\mu}\right) - \sum_{\alpha=1}^{N}\vec{c}_\alpha\frac{\partial h_\alpha(\phi)}{\partial t} - \sum_{\alpha=1}^{N} h_\alpha(\vec{\phi})\left(\frac{\partial\vec{c}_\alpha}{\partial T}\right)\frac{\partial T}{\partial t}\right)$$

Hötzer et al. Phase-field simulation of solid state sintering, Acta Materialia (2018)

Phase-field model for solid state sintering

- **phase-field model** based on grand potential approach
  - evolution of phase-fields $\partial_t \phi_\alpha$
  - evolution of chemical potentials $\partial_t \boldsymbol{\mu}$
  - constant temperature
- different **diffusion mechanisms**: surface (5), grain boundary (2) and volume diffusion (1,3,4,6)
- **arbitrary** number **phases/grains**
- **optimized** on different levels
- massive-parallel PACE3D framework

⇒ **efficient simulation** of large domains

$$\tau\varepsilon\frac{\partial\phi_\alpha}{\partial t} = \underbrace{-\varepsilon\left(\frac{\partial a(\phi,\nabla\phi)}{\partial\phi_\alpha} - \nabla\cdot\frac{\partial a(\phi,\nabla\phi)}{\partial\nabla\phi_\alpha}\right) - \frac{1}{\varepsilon}\frac{\partial\omega(\phi)}{\partial\phi_\alpha}}_{\text{interface contribution } :=\text{rhsI}_\alpha}$$

$$\underbrace{-\frac{\partial\psi(\phi,\boldsymbol{\mu},T)}{\partial\phi_\alpha}}_{\text{driving force } :=\text{rhsf}_\alpha} - \frac{1}{N}\sum_{\beta=1}^{N}(\text{rhsI}_\beta + \text{rhsf}_\beta)$$

$$\frac{\partial\boldsymbol{\mu}}{\partial t} = \left[\sum_{\alpha=1}^{N} h_\alpha(\vec{\phi})\left(\frac{\partial\vec{c}_\alpha(\boldsymbol{\mu},T)}{\partial\boldsymbol{\mu}}\right)\right]^{-1} \left(\nabla\cdot\left(\boldsymbol{M}(\vec{\phi},\boldsymbol{\mu},T)\nabla\boldsymbol{\mu}\right) - \sum_{\alpha=1}^{N}\vec{c}_\alpha\frac{\partial h_\alpha(\phi)}{\partial t} - \sum_{\alpha=1}^{N} h_\alpha(\vec{\phi})\left(\frac{\partial\vec{c}_\alpha}{\partial T}\right)\frac{\partial T}{\partial t}\right)$$

Hötzer et al. Phase-field simulation of solid state sintering, Acta Materialia (2018)

Phase-field model for solid state sintering

- **phase-field model** based on grand potential approach
  - evolution of phase-fields $\partial_t \phi_\alpha$
  - evolution of chemical potentials $\partial_t \boldsymbol{\mu}$
  - constant temperature
- different **diffusion mechanisms**: surface (5), grain boundary (2) and volume diffusion (1,3,4,6)
- **arbitrary** number **phases/grains**
- **optimized** on different levels
- massive-parallel PACE3D framework

⇒ **efficient simulation** of large domains

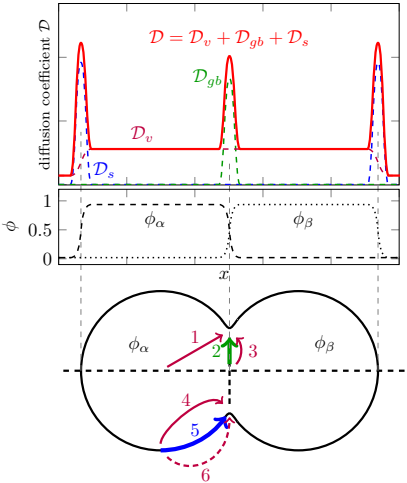

Hötzer et al. Phase-field simulation of solid state sintering, Acta Materialia (2018)

Phase-field model for solid state sintering

- **phase-field model** based on grand potential approach
  - evolution of phase-fields $\partial_t \phi_\alpha$
  - evolution of chemical potentials $\partial_t \boldsymbol{\mu}$
  - constant temperature
- different **diffusion mechanisms**: surface (5), grain boundary (2) and volume diffusion (1,3,4,6)
- **arbitrary** number **phases/grains**
- **optimized** on different levels
- massive-parallel PACE3D framework

⇒ **efficient simulation** of large domains

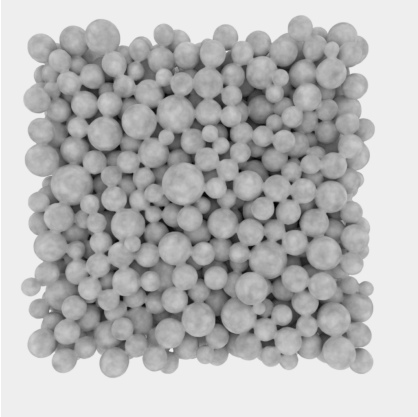

Hötzer et al. The parallel multi-physics phase-field framework Pace3D, Journal of computational science 26 (2018)

Phase-field model for solid state sintering

- **phase-field model** based on grand potential approach
  - evolution of phase-fields $\partial_t \phi_\alpha$
  - evolution of chemical potentials $\partial_t \boldsymbol{\mu}$
  - constant temperature
- different **diffusion mechanisms**: surface (5), grain boundary (2) and volume diffusion (1,3,4,6)
- **arbitrary** number **phases/grains**
- **optimized** on different levels
- massive-parallel PACE3D framework

⇒ **efficient simulation** of large domains

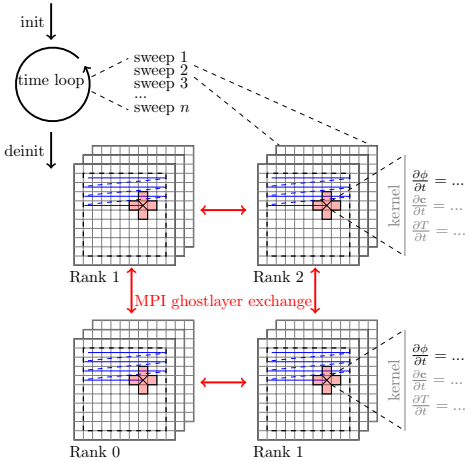

Hötzer et al. The parallel multi-physics phase-field framework Pace3D, Journal of computational science 26 (2018)

Phase-field model for solid state sintering

- **phase-field model** based on grand potential approach
  - evolution of phase-fields $\partial_t \phi_\alpha$
  - evolution of chemical potentials $\partial_t \boldsymbol{\mu}$
  - constant temperature
- different **diffusion mechanisms**: surface (5), grain boundary (2) and volume diffusion (1,3,4,6)
- **arbitrary** number **phases/grains**
- **optimized** on different levels
- massive-parallel PACE3D framework

⇒ **efficient simulation** of large domains

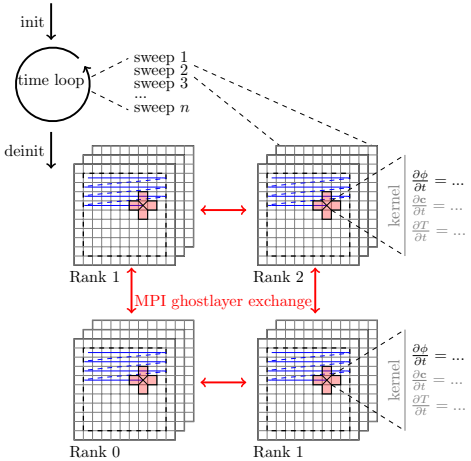

Phase-field model for solid state sintering

- **phase-field model** based on grand potential approach
  - evolution of phase-fields $\partial_t \phi_\alpha$
  - evolution of chemical potentials $\partial_t \boldsymbol{\mu}$
  - constant temperature
- different **diffusion mechanisms**: surface (5), grain boundary (2) and volume diffusion (1,3,4,6)
- **arbitrary** number **phases/grains**
- **optimized** on different levels
- massive-parallel PACE3D framework

$\Rightarrow$ **efficient simulation** of large domains

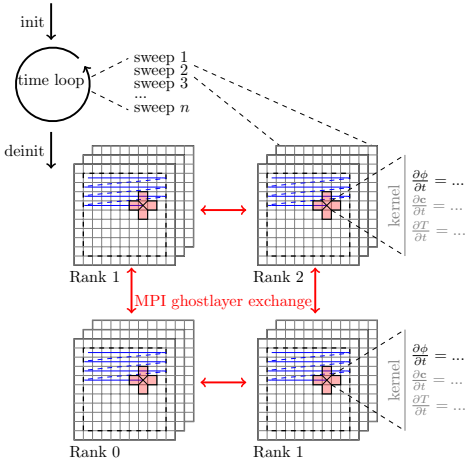

Part IV: Implementation of the phase-field model

https://www.flickr.com/photos/149836801@N02/35401845633/

Phase-field algorithm

- lattice fields
  - two AoS for phase-field (ϕ_{src}, ϕ_{dst})
  - two SoA for chemical potential ($\boldsymbol{\mu}_{src}$, $\boldsymbol{\mu}_{dst}$)
  - communication hiding for both sweeps
- storing new values calculated from *src* in *dst*

Algorithm 1 time step with overlapping communication

1: END: COMMUNICATION (ϕ_{src})
2: $\quad \boldsymbol{\phi_{dst}} \leftarrow \phi$**-sweep**$\left(\boldsymbol{\phi_{src}}, \boldsymbol{\mu_{src}}\right)$
3: $\quad \phi_{dst}$-BOUNDARY CONDITIONS
4: START: COMMUNICATION (ϕ_{dst})
5: END: COMMUNICATION ($\boldsymbol{\mu}_{src}$)
6: $\quad \boldsymbol{\mu_{dst}} \leftarrow \mu$**-sweep**$\left(\boldsymbol{\mu_{src}}, \boldsymbol{\phi_{src}}, \boldsymbol{\phi_{dst}}\right)$
7: $\quad \boldsymbol{\mu}_{dst}$-BOUNDARY CONDITIONS
8: START: COMMUNICATION ($\boldsymbol{\mu}_{dst}$)
9: $\quad$ SWAP $\phi_{src} \leftrightarrow \phi_{dst}$ and $\boldsymbol{\mu}_{src} \leftrightarrow \boldsymbol{\mu}_{dst}$

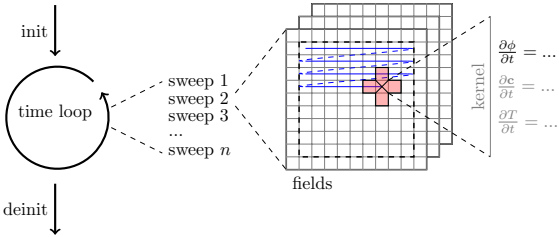

ϕ-sweep

$$\tau\varepsilon\frac{\partial\phi_\alpha}{\partial t} = \underbrace{-\varepsilon\left(\frac{\partial a(\phi,\nabla\phi)}{\partial\phi_\alpha} + \nabla\cdot\frac{\partial a(\phi,\nabla\phi)}{\partial\nabla\phi_\alpha}\right)}_{\text{D3C7}} \underbrace{-\frac{1}{\varepsilon}\frac{\partial\omega(\phi)}{\partial\phi_\alpha} - \frac{\partial\psi(\phi,\boldsymbol{\mu})}{\partial\phi_\alpha} + \lambda}_{\text{D3C1}}$$

- finite differences scheme for space
- forward Euler scheme for the time discretization
- local reduction of order-parameters with size 8
  $\Rightarrow$ handle arbitrary number of evolution equations at cost of using lookup table for values

$$\phi(\mathbf{x},t) \xrightarrow{\text{D3C7}} \phi(\mathbf{x},t+\Delta t)$$

$$\mu(\mathbf{x},t) \xrightarrow{\text{D3C1}}$$

index	value	e.g.
$N-1$	ϕ_{N-1}	0
$N-2$	ϕ_{N-2}	0
$N-3$	ϕ_{N-3}	0.57
$\vdots$		$\vdots$
2	ϕ_2	0
1	ϕ_1	0.43
0	ϕ_0	0

$\rightarrow$

index	value	e.g.	
-	-	-	-
-	-	-	-
-	-	-	-
-	-	-	-
N − 3	ϕ_{N-3}	N − 3	0.57
1	ϕ_1	1	0.43

μ-sweep

$$\frac{\partial \boldsymbol{\mu}}{\partial t} = \underbrace{\left[\sum_{\alpha=1}^{N} h_\alpha(\vec{\phi}) \left(\frac{\partial \vec{c}^\alpha(\boldsymbol{\mu})}{\partial \boldsymbol{\mu}}\right)\right]^{-1}}_{\text{D3C1}} \left(\underbrace{\nabla \cdot \left(\boldsymbol{M}(\vec{\phi}, \boldsymbol{\mu}) \nabla \boldsymbol{\mu}\right)}_{\text{D3C7}} - \underbrace{\sum_{\alpha=1}^{N} \vec{c}^\alpha(\boldsymbol{\mu}) \frac{\partial h_\alpha(\boldsymbol{\phi})}{\partial t}}_{\text{D3C1}}\right)$$

- finite differences scheme for space
- forward Euler and implizit scheme for the time discretization

$$\begin{tikzcd}
\phi(\mathbf{x}, t) \arrow[dr, "\text{D3C7}"] & \phi(\mathbf{x}, t + \Delta t) \arrow[d, "\text{D3C1}"] \\
\mu(\mathbf{x}, t) \arrow[r, "\text{D3C7}"'] & \mu(\mathbf{x}, t + \Delta t)
\end{tikzcd}$$

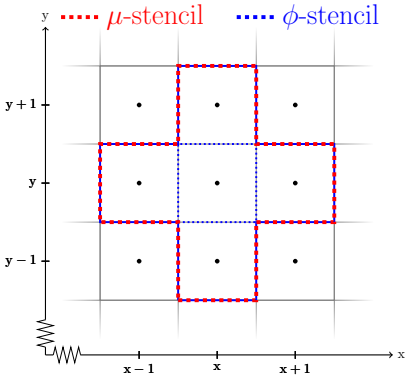

Part V: Optimizations

Optimizations

Parameter layer

- fitted parabolic Gibbs energies
- reduction of the parameter matrices to a class based concept

Model layer

- classification of cells
  $\Rightarrow$ skip terms
- pre-calculation of values
- scalar mobility function instead of tensor mobility

Numeric layer

- $\partial_t \phi \Rightarrow$ forward Euler scheme
- $\partial_t \mu \Rightarrow$ forward Euler scheme, Jacobi, PCG

Algorithm layer

- streaming in sweeps
- advanced buffering techniques
- domain decomposition (MPI)
- communication hiding
- local reduction of order parameter (LROP) of the N element ϕ-vector to 8 elements
- MPI-IO and reduced mesh output

Hardware layer

- explicit vectorization of kernels
- optimized memory layouts (AoS vs. SoA)

Optimizations

Numerical layer

- diffusion coefficient differs over multiple order of magnitude
- ϕ-equ. operates on larger stable time step width as μ-equ.
- μ-equ. is relatively localized and well-conditioned

  $\Rightarrow$ different implicit scheme to solve μ-equ.
  - Jacobi (JAC)
  - Jacobi with fixed number of iterations (JACFIX*N*)
  - preconditioned conjugated gradient method (PCG)

  $\Rightarrow$ explicit forward euler scheme to solve ϕ-equ.

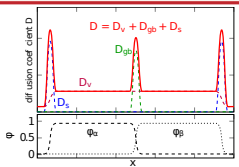

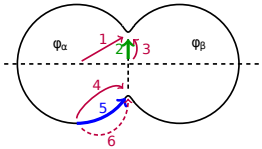

Part VI: Performance results

https://www.flickr.com/photos/135366503N05/27140651174/

Roofline

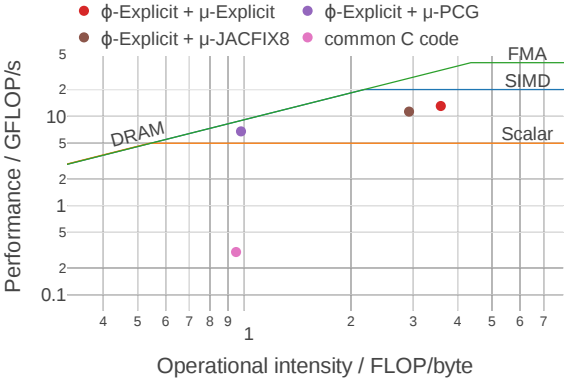

- PCG 646 times and JACFIX8 1736 faster than the common explicit C-code
- ϕ-Explicit + μ-Explicit $\Rightarrow$ 32.5 %
- ϕ-Explicit + μ-JACFIX8 $\Rightarrow$ 28.2 %
- ϕ-Explicit + μ-PCG $\Rightarrow$ 16.9 %

- Hazel Hen - 2x 12 core Intel Xeon CPU E5-2680 v3
- frequency pinned to 2.5 Ghz
- single core result
- 80^3 voxel cell

Hierl, Hötzer, Seiz et al. Extreme Scale Phase-Field Simulations of Sintering Processes, IEEE/ACM scalA (2019)

Single node scaling

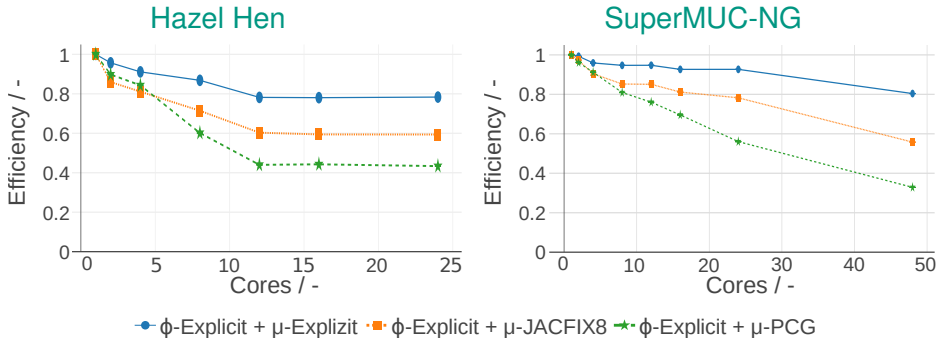

- drop due to saturation of memory bandwidth
- implicit scheme scale worse
- time to solution for implicit scheme still much smaller

$\Rightarrow$ further cache and memory optimizations needed

- Hazel Hen - 2x 12 core Intel Xeon CPU E5-2680 v3
- SuperMUC-NG - 2x 24 core Intel Skylake Xeon Platinum 8174
- 80^3 voxel cell per rank
- frequency pinned to 2.5 Ghz
- $\Delta t_\phi = 40 \Delta t_\mu$

Hierl, Hötzer, Seiz et al. Extreme Scale Phase-Field Simulations of Sintering Processes, IEEE/ACM scalA (2019)

Weak scaling results

Hazel Hen

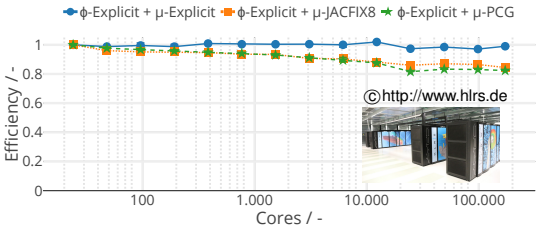

SuperMUC-NG

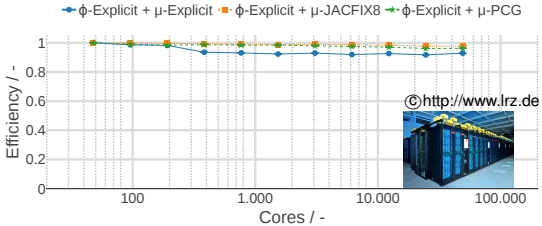

- Hazel Hen - 2x 12 core Intel Xeon CPU E5-2680 v3
- 185 088 cores ⇒ 7.4 PFlops
- SuperMUC-NG - 2x 24 core Intel Skylake Xeon Platinum 8174
- 304 128 core ⇒ 26.3 PFlops
- 80^3 voxel cell per rank
- $\Delta t_\phi = 40 \Delta t_\mu$

- proper weak scaling behavior up to 170 000 cores for all schemes

Hierl, Hötzer, Seiz et al. Extreme Scale Phase-Field Simulations of Sintering Processes, IEEE/ACM scalA (2019)

Strong scaling results

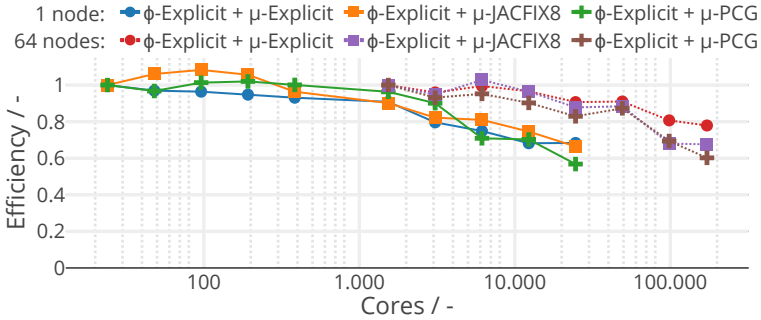

- for $> 50^3$ voxel cell domain per process:
  $\Rightarrow$ efficiency $> 70\,\%$ compared to single node
- abnormal scaling behavior probably due to domain decomposition effect

- Hazel Hen - 2x 12 core Intel Xeon CPU E5-2680 v3
- 185 088 cores $\Rightarrow$ peak performance: 7 420 TFlops
- two settings (**1N** and **64N**), memory almost entirely used

  1N starting from 1 node with $640 \times 480 \times 640$ voxel cells

  64N starting from 64 nodes with $1\,920 \times 6\,720 \times 1\,280$ voxel cells
- $\Delta t_\phi = 40 \Delta t_\mu$

Hierl, Hötzer, Seiz et al. Extreme Scale Phase-Field Simulations of Sintering Processes, IEEE/ACM scalA (2019)

Strong scaling results

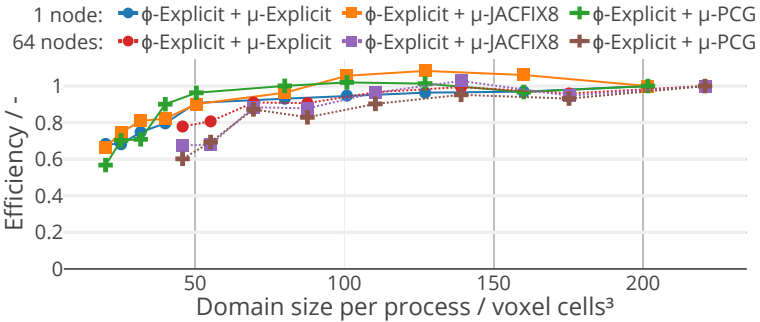

- for $> 50^3$ voxel cell domain per process:
  $\Rightarrow$ efficiency $> 70\,\%$ compared to single node
- abnormal scaling behavior probably due to domain decomposition effect

- Hazel Hen - 2x 12 core Intel Xeon CPU E5-2680 v3
- 185 088 cores $\Rightarrow$ peak performance: 7 420 TFlops
- two settings (**1N** and **64N**), memory almost entirely used

  1N starting from 1 node with $640 \times 480 \times 640$ voxel cells

  64N starting from 64 nodes with $1\,920 \times 6\,720 \times 1\,280$ voxel cells
- $\Delta t_\phi = 40 \Delta t_\mu$

Hierl, Hötzer, Seiz et al. Extreme Scale Phase-Field Simulations of Sintering Processes, IEEE/ACM scalA (2019)

Time to solution (TTS) comparison – Hazel Hen

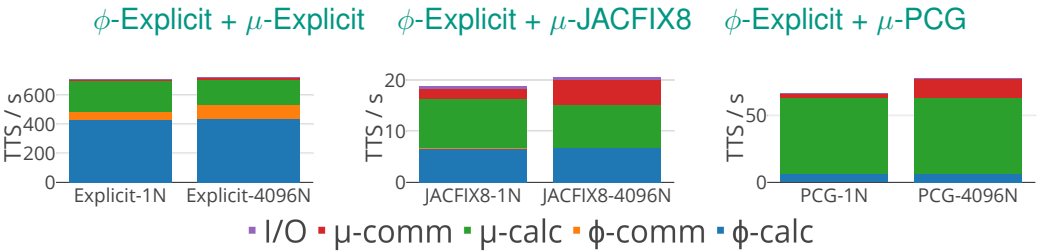

- implicit schemes are much faster as explicit ones
- slight increase for JACFIX8 and PCG in TTS
- μ-communication hidden in explicit case
- ϕ-communication hidden in implicit cases
- in implicit cases μ-communication increases

- Hazel Hen - 2x 12 core Intel Xeon CPU E5-2680 v3
- **comparison** between one **1 node (*-1N)** and **4096 nodes (*-4096N)**
- $\Delta t_\phi = 40 \Delta t_\mu$

Hierl, Hötzer, Seiz et al. Extreme Scale Phase-Field Simulations of Sintering Processes, IEEE/ACM scalA (2019)

I/O optimizations

- MPI-I/O to store voxel fields for
  - detailed analysis
  - checkpointing

$\Rightarrow$ $\sim 90\ {}^{GB}/_{s} \longleftrightarrow 44.5\,\%$ peak performance[a]

- reduced mesh output based on STL format for
  - analysis
  - visualization

$\Rightarrow$ $\sim 142\ {}^{GB}/_{s} \longleftrightarrow 71\,\%$ peak performance[b]

$\Rightarrow$ $\sim$ MB for STL instead of
$\sim$ GB for voxel fields

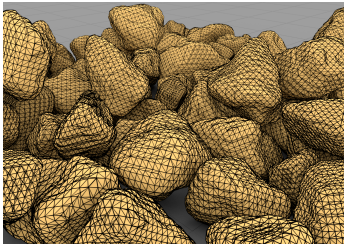

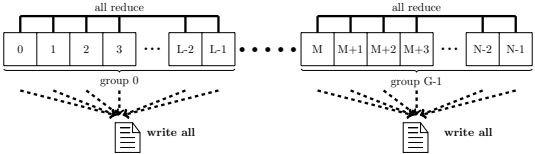

[a] $2\,400^3$ voxel = 823GB, 6 144 cores, 1728 writter on 54 OST using HLRS WS9 file system

[b] $2\,400^3$ voxel, 6 144 cores, 54 MPI groups writting 193GB on HLRS WS9 file system in 3.5s including marching

Part VII: Simulation results of the sintering process

Setting for 3D simulations

- 3D simulations based on parameters of Al_2O_3
- $400 \times 400 \times 400$ voxel cell domain
- 24 897 particles with a radius of 0.35 µm
- initial density 63.8 %
- calculations on 1 083 cores of Hazel Hen supercomputer for 50h
- 10 million time steps
- different active diffusion mechanisms
  - D_v
  - $D_v + D_{gb}$
  - $D_v + D_s$
  - $D_v + D_{gb} + D_s$

- note: grain growth artificially inhibited for comparison with Coble model

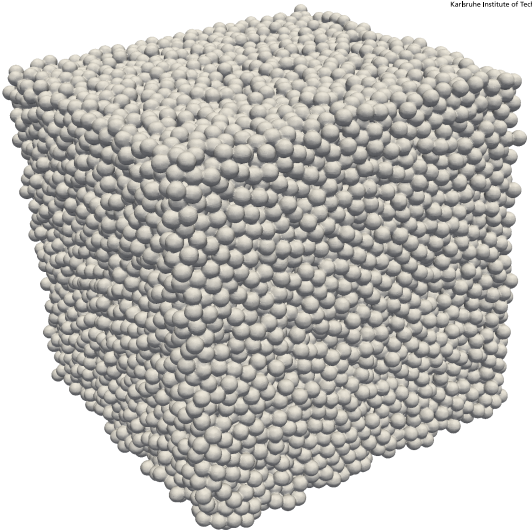

Hötzer et al. Phase-field simulation of solid state sintering, Acta Materialia (2018)

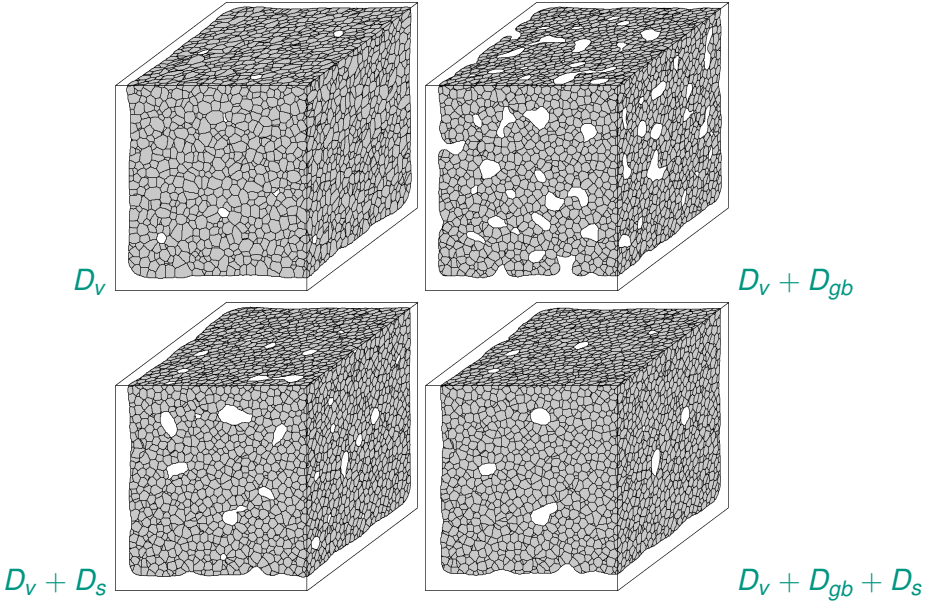

Hötzer et al. Phase-field simulation of solid state sintering, Acta Materialia (2018)

Extreme scale simulation

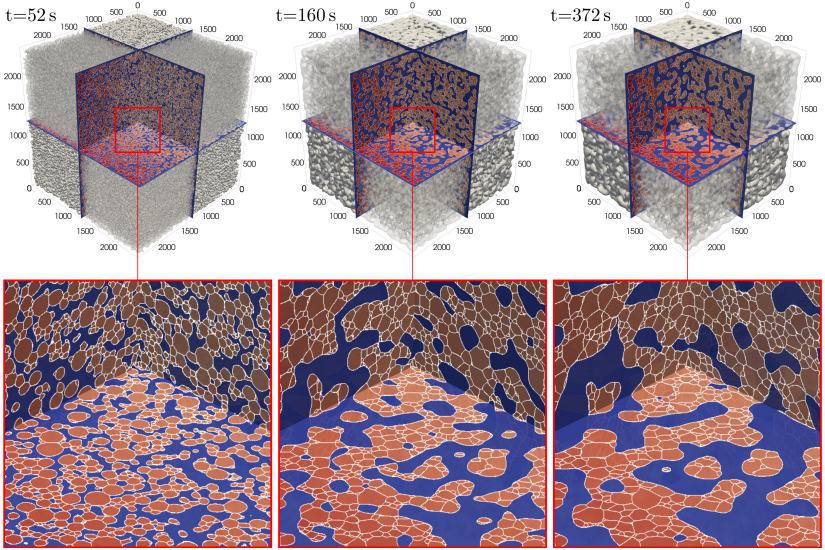

- parameters based on Al_2O_3
- with $D_s = D_{gb} = 1\,000 \cdot D_v$
- $2\,400 \times 2\,400 \times 2\,400$ voxel cells
  $\Rightarrow 120 \times 120 \times 120 \mu m$
- initially packed with 1 191 901 individual particles
- computed with 168 000 cores of the Hazel Hen supercomputer

Hierl, Hötzer, Seiz et al. Extreme Scale Phase-Field Simulations of Sintering Processes, IEEE/ACM scalA (2019)

Conclusions

- synergistic optimizations provided a 31-fold improvement for the explicit scheme
- implicit schemes 620 (PCG) and 1 736 (JACFIX8) faster than common C code
- up to 32.5 % single-core peak performance
- mostly ideal weak-scaling behavior of explicit and implicit schemes in multi node case
- up to 24.5 % peak performance on 98 304 cores

- ability to:
  - solve the phase-field equation for millions of unknowns
  - efficiently calculate huge domains
- both of which are necessary to resolve realistic particle size distributions over multiple orders of magnitude (nm—μm)
- allows improving the understanding of sintering materials as well as the formation of glaciers

$\Rightarrow$ **wholistic optimizations and parallelization** enable the investigation of realistic microstructures

Visit me also at Poster 77

Open questions? Ideas? Improvements?

- Johannes Hötzer: johannes.hoetzer@kit.edu
- Britta Nestler: britta.nestler@kit.edu

Visit me also at Poster 77